POLYMER-BASED S-SHAPED WAVEGUIDE VOA FOR APPLICATIONS IN THE BROADBAND DWDM NETWORK

Ying-Tsung Lu,[1,2] Huang-Chen Guo,[2] Hseng-Tsong Wang,[1] and Sien Chi[1]
[1] Institute of Electro-Optical Engineering
National Chiao-Tung University
1001 Ta Hsueh Rd.
Hsinchu, Taiwan 300, R.O.C.
[2] Opto-Electronics & Systems Laboratories
Industrial Technology Research Institute
Chung Hsing Rd.
Chutung, Hsinchu, Taiwan 310, R.O.C.

Received 13 March 2003

ABSTRACT: *A polymer-based thermal-controllable waveguide variable optical attenuator (VOA) is proposed. We numerically design an S-shaped buried waveguide structure with a polymer core and silica cladding, which can attenuate light with satisfactory optical attenuation in the spectrum range from 1.28 to 1.58 μm. The design is suitable for the integration of VOAs with planar lightwave devices and is easy to fabricate as monolithic optical modules for application in optical communication systems.* © 2003 Wiley Periodicals, Inc.
Microwave Opt Technol Lett 39: 1–4, 2003; Published online in Wiley InterScience (www.interscience.wiley.com). DOI 10.1002/mop.11108

Key words: *variable optical attenuator; thermal-optical effect; optical attenuation; polymer waveguide*

1. INTRODUCTION

The variable optical attenuator (VOA) has been widely used to modulate the light power automatically in a long-haul or local network. It has also become an important device to equalize the channels' light power in order to avoid switching crosstalk and power fluctuation in a DWDM communication system. The attenuation induced from either the Electro-Optical effect or the separation of fiber connection is usually used to fabricate a VOA [1]. Moreover, MEMS technology is also employed for the VOA fabrication [2]. However, most of these methods suffer from either high cost or high optical loss in operation.

In recent years, the development of VOA using a planar lightwave circuit (PLC) was proposed [3–6]. It can be integrated with an AWG or OADM device for a valuable monolithic optical module with low cost and compact size. However, the VOAs based on the Y-branch and Mach–Zehnder types of waveguides both have the disadvantage of the low ratio of light-attenuation to size (power/mm). This drawback leads to a large-size VOA. According to the requirement of the optical attenuation of 15–25 dB in a DWDM system, only the waveguide VOAs with a high ratio of light-attenuation to size have the potential to be integrated with present planar waveguide components for the fabrication of novel communication devices with satisfactory functions. One of the attractive waveguide materials is polymer, which was used to fabricate the optical communication devices [7–9]. Its thermal-optical property was employed to fabricate the thermal-controllable VOA [10–11]. The manufacturing process for a polymer-based VOA is simpler than that for a silica-based VOA and therefore can lower the cost of fabrication. The VOA application of using a polymer PLC with a bending structure has been demonstrated [12]. However, the single bending structure is inefficient for light attenuation in the waveguide; therefore, long waveguide length is required in the application.

In this paper, we propose a compact polymer waveguide VOA with an S-shaped structure. Its double bending design, incorporated with the thermal-optical property of polymer, provides optimal optical attenuation within a small waveguide length. We numerically show that the attenuations for the wavelength range of 1.28–1.3 μm and 1.51–1.56 μm are larger than 20 and 30 dB, respectively. In addition, the attenuations of the waveguide with various bending curvatures are simulated. The attenuations versus TE and TM modes in the windows of 1.3 μm and 1.5 μm are also evaluated.

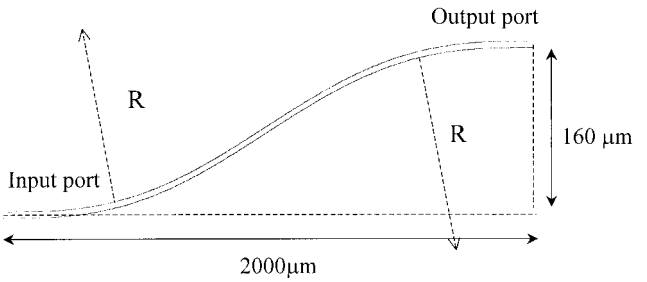

Figure 2 S-shaped waveguide structure with R the radius of the bending curvature

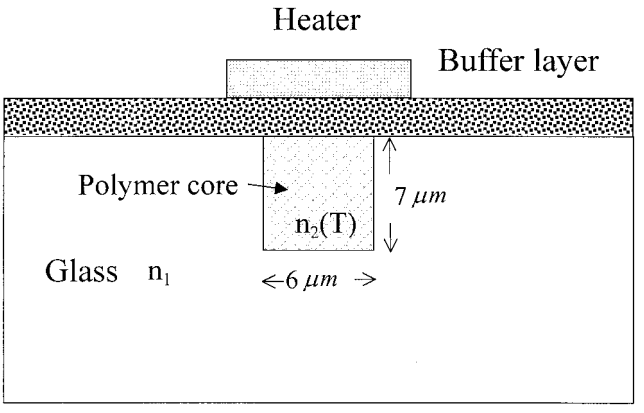

Figure 1 Cross section of the waveguide VOA

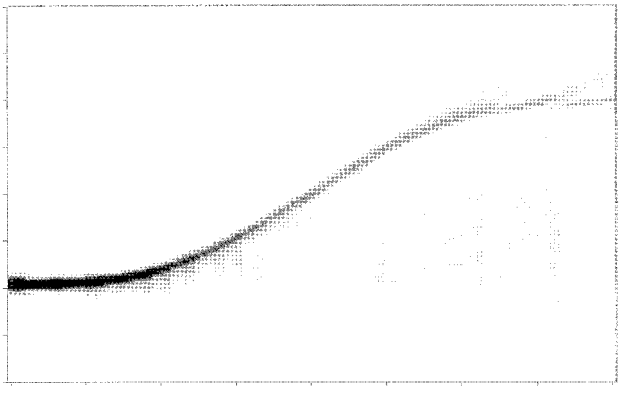

Figure 3 Field distribution of the S-shaped waveguide VOA at R = 4430 μm

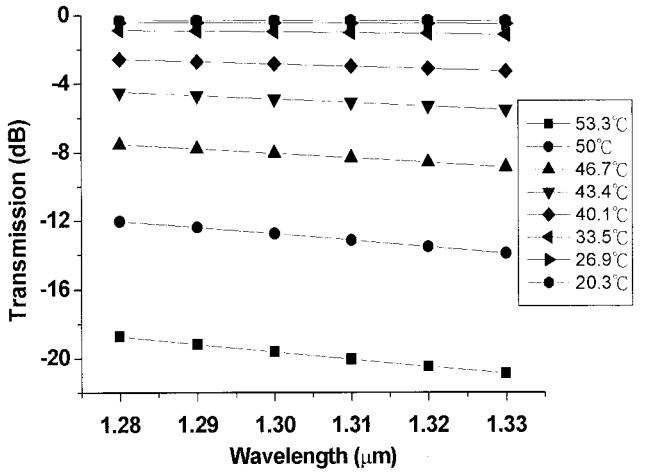

Figure 4 Simulated attenuation in wavelength range 1.28–1.33 μm for various temperatures at $R = 4430$ μm

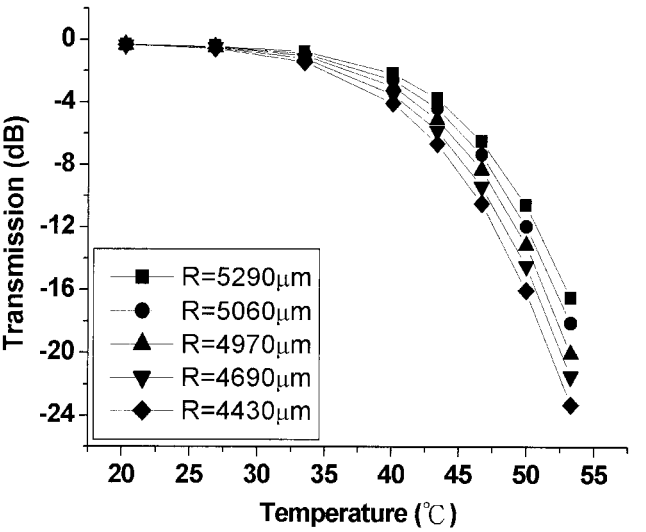

Figure 6 Simulated attenuation of the mode at 1310 nm versus temperature for different waveguide curvatures

2. PRINCIPLE

Figure 1 schematically shows the cross section of the S-shaped waveguide VOA. It can be fabricated by dry etching the rectangular groove on the top of the silica substrate and then spin coating the polymer on the substrate to fill out the groove for the core of the waveguide. A buffer layer is subsequently coated on the top of the buried core in order to separate the metal heater from the core layer. The buried-type waveguide with polymer core and silica cladding provides satisfactory index tuning contrast between the core and cladding under thermal variation. The design principle of the optical loss mechanism in such a buried-type S-shaped waveguide VOA is based on the index variation of the core under a change in temperature. The effective index of the fundamental mode will be changed, while the refractive index of the core is varied. Consequently, the field distribution of the mode inside the core is changed. The tuning range of the thermal-dependent index of the polymer determines the variation of the mode field. Moreover, the bending design of the waveguide enhances the attenuation to fit the requirements of a DWDM network. The design of the S-shaped structure is shown in Figure 2. The power loss of the bending waveguide VOA is expressed as [13]:

$$P_{loss} = \frac{2\gamma\alpha^2 \cdot e^{2\gamma t} \cdot e^{-(2/3)\cdot\gamma^3 R/\beta^2}}{[n_2^2(T) - n_1^2] \cdot k^2 \beta (2t + 2/\gamma)}$$

where $\alpha = [n_2^2(T)k^2 - \beta^2]^{1/2}$, $\gamma = (\beta^2 - n_1^2 k^2)^{1/2}$, $k = \omega(\varepsilon_0\mu_0)^{1/2} = 2\pi/\gamma$ is the wave number, $\omega = 2\pi f$ is the angular frequency, β is the propagation constant, $2t$ is the width of the waveguide, n_1 is the refractive index of cladding region, $n_2(T)$ is the thermal dependent refractive index of the core, ε_0 is the electric permittivity of free space, μ_0 is the magnetic permeability of free space, and R is the radius of bending. In general, the thermal-optical parameter (dn/dT) of polymer is in the scale of -1.5–-3×10^{-4}/°C. Therefore, the index of the polymer core should be as close as possible to that of cladding substrate; more efficient mode-field variation can be obtained under the change of temperature. However, if the polymer with a large thermal-optical parameter is used as the core material, glasses with a large index difference from that of core may also be employed as the cladding substrate. Silica is chosen as the cladding material because its

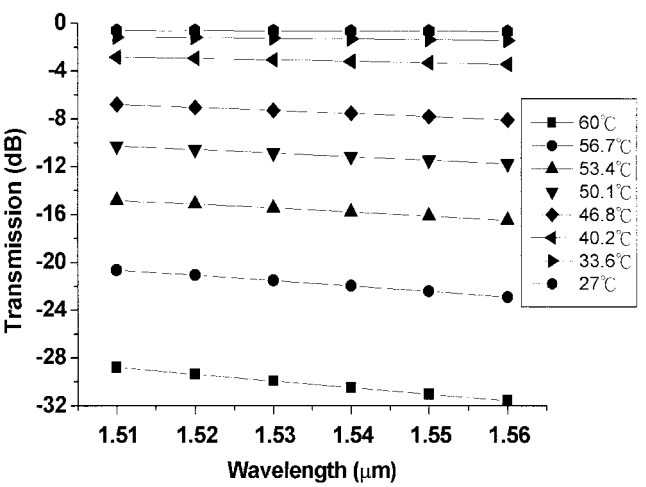

Figure 5 Simulated attenuation in wavelength range from 1.51 to 1.56 μm for various temperatures at $R = 4430$ μm

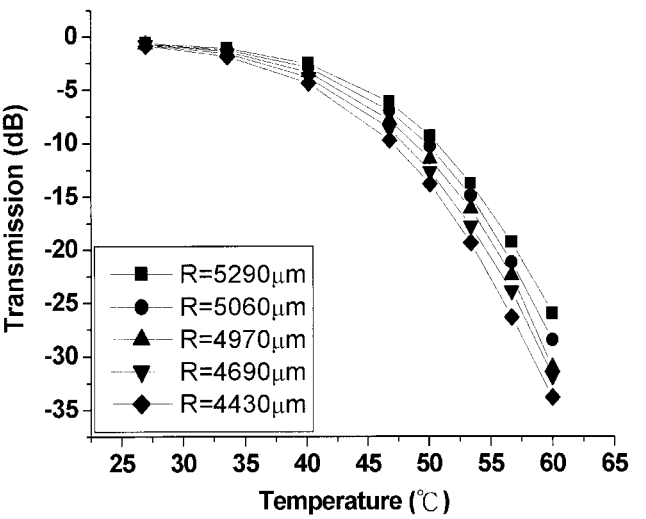

Figure 7 Simulated attenuation of the mode at 1550 nm versus temperature for different waveguide curvatures

index is changed with a rate of less than 10^{-6}/°C. This means that an efficient index contrast is obtained between the core and cladding under thermal variation.

3. SIMULATION AND DISCUSSION

The polymer with the potential to fabricate the core of the VOA, BCB4024 from Dow Chemical Company, has a refractive index of 1.542. The measured dn/dT value is -1.5×10^{-4}/°C. The Bak_2 glass wafer, from Schott Company, has an index of 1.526 and is used as the cladding substrate. As shown in Figures 1 and 2, the core of the waveguide is designed to be S-shaped with a width of 7 μm and height of 6 μm, which is the proper cross section for adjusting the confinement of the mode field in order to control the radiation loss. The vertical displacement of the output and input ports is 160 μm, and is 2000 μm in the horizontal direction. The three-dimensional (3D) beam-propagation method is used to simulate the beam propagation and the attenuation of the waveguide by using the abovementioned processes and materials. The field that distributes inside and outside the waveguide is shown as Figure 3. In the spectrum range from 1.28 to 1.33 μm, the light-power attenuation of the core mode versus temperature varied from 20.3°C to 57.3°C, as shown in Figure 4. In the C-band (1.51–1.56 μm), the attenuation versus temperature varied from 27°C to 60°C, as shown in Figure 5. The light power is attenuated regularly with respect to the variation of temperature through the spectrum at 1.28 to 1.33 μm, and 1.51 to 1.56 μm. However, the attenuation levels are inclined at high temperatures. This can be compensated by using an electric circuit to modulate the temperature for different transmission channels in the applications of a DWDM network. The power attenuations for the mode at the windows of 1.31 μm and 1.5 μm versus different bending curvatures under temperature variation are shown in Figures 6 and 7, respectively. The attenuation becomes larger when the curvature of the waveguide is increased. The attenuations of TE and TM modes in the spectrum at 1.28 to 1.33 μm, and that from 1.51 to 1.56 μm, are shown in Figures 8 and 9, respectively. It was found there are no substantial attenuation difference between the TE and TM modes in the spectrum windows of 1.3 μm and 1.5 μm.

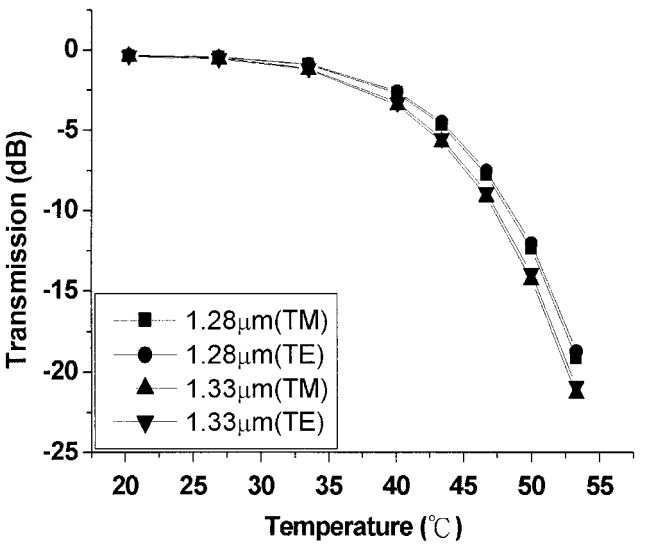

Figure 8 Attenuation of TE and TM modes versus temperature at wavelengths of 1.28 μm and 1.33 μm (R = 4430 μm)

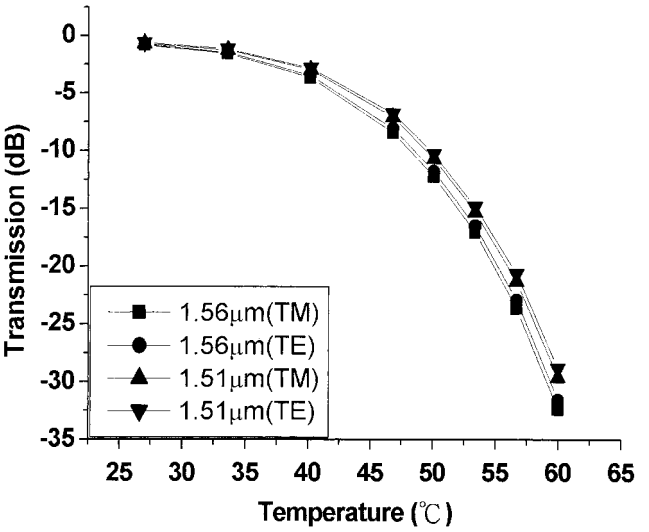

Figure 9 Attenuation of TE and TM modes versus temperature at wavelengths of 1.51 μm and 1.56 μm (R = 4430 μm)

4. CONCLUSION

A compact S-shaped polymer-based waveguide, suitable for fabricating a VOA, has been demonstrated. The simulated results of power attenuation up to 20 and 30 dB in optical communication windows of 1.31 and 1.55 μm have been presented, respectively. We have shown that the power attenuation is independent of the polarization state of the propagation beam, and the proposed polymer waveguide VOA can attenuate light beam without PDL. This compact design is suitable for the integration of VOAs and fiber or PLC devices for application in a broadband communication system. Its simple manufacturing process adds to its potential as a low-cost device that will accommodate the future requirements of long-haul and local networks.

REFERENCES

1. K. Hibayashi, M. Wada, and C. Amano, Liquid crystal variable optical attenuators integrated on planar lightwave circuits, IEEE Photon Technol Lett 13 (2001), 609–611.
2. W. Noell, P.A. Clerc, L. Dellmann, B. Guldimann, H.P. Herzig, O. Manzardo, C.R. Marxer, K.J. Weible, R. Dandliker, and N. Rooij, Applications of SOI-based optical MEMS, IEEE J Sel Topics Quantum Electron 8 (2002), 148–154.
3. M. Lenzi, S. Tebaldini, D.D. Mola, S. Brunazzi, and L. Cibinetto, Power control in the photonic domain based on integrated arrays of optical variable attenuators in glass-on-silicon technology, IEEE J Sel Topics Quantum Electron 5 (1999), 1289–1297.
4. S.S. Lee, Y.S. Jin, Y.S. Son, and T.K. Yoo, Polymeric tunable optical attenuator with an optical monitoring tap for WDM transmission network, IEEE Photon Technol Lett 11 (1999), 590–592.
5. S.S. Lee, Y.S. Jin, and Y.S. Son, Variable optical attenuator based on a cutoff modulator with tapered waveguide in polymers, J Lightwave Technol 17 (1999), 2556–2561.
6. L. Eldada and L.W. Shacklette, Advances in polymer integrated optics, IEEE J Selected Topics Quantum Electron 6 (2000), 54–68.
7. C.F. Kane and R.R. Krchnavek, Benzocyclobutene optical waveguides, IEEE Photon Technol Lett 7 (1995), 535–537.
8. C.F. Kane and R.R. Krchnavek, Processing and characterization of benzocyclobutene optical waveguides, IEEE Trans Comp Packag Manufact Technol B 18 (1995), 565–571.
9. N. Keil, H.H. Yao, C. Zawadzki, J. Bauer, M. Bauer, C. Dreyer, J. Schneider, Athermal all-polymer arrayed-waveguide grating multiplexer, Electronics Letters, 37 (2001), 579–580.
10. Y.O. Noh, M.S. Yang, Y.H. Won, W.Y. Hwang, PLC-type variable

optical attenuator operated at low electric power, Electronics Letters 36 (2000), 579–580.
11. T.C. Kowalczyk, I. Finkelshtein, M. Kouchnir, Y.C. Lee, A.D. Nguyen, D. Vroom, W.K. Bischel, Variable optical attenuator with large dynamic range and low drive power, Optical Fiber Communication Conference and Exhibit, OFC 2001 3 (2001), WR-1–4.
12. S.M. Garner, S. Caracci, Variable optical attenuation for large-scale integration, IEEE Photon Technol Lett 14 (2002), 1560–1562.
13. D. Marcuse, bending losses of the asymmetric slab waveguide, BSTJ 50 (1971), 2551–2563.

NF–FF TRANSFORMATION WITH CYLINDRICAL SCANNING FROM NONUNIFORMLY DISTRIBUTED DATA

F. Ferrara,[1] C. Gennarelli,[1] G. Riccio,[1] and C. Savarese[2]
[1] Dipartimento di Ingegneria dell'Informazione ed Ingegneria Elettrica
University of Salerno
via Ponte Don Melillo
I-84084 Fisciano, Salerno, Italy
[2] Istituto di Teoria e Tecnica delle Onde Elettromagnetiche
University of Naples "Parthenope"
via Acton
80133 Naples, Italy

Received 6 March 2003

ABSTRACT: *Two efficient probe-compensated near-field–far-field (NF–FF) transformation techniques with cylindrical scanning requiring a minimum number of irregularly spaced data, are proposed. Singular value decomposition (SVD) method is applied to evaluate the uniformly distributed samples, whose positions are fixed by a nonredundant sampling representation of the field, from the irregularly spaced ones. Then, the voltage data needed by standard NF–FF transformation or by a non-conventional one recently developed by the authors are efficiently evaluated via an optimal sampling interpolation algorithm.* © 2003 Wiley Periodicals, Inc. Microwave Opt Technol Lett 39: 4–8, 2003; Published online in Wiley InterScience (www.interscience.wiley.com). DOI 10.1002/mop.11109

Key words: *NF–FF transformation techniques; probe compensation; cylindrical scanning; nonredundant sampling representations; nonuniform sampling*

1. INTRODUCTION

Among the near-field–far-field (NF–FF) transformation techniques, cylindrical scanning is particularly attractive. In fact, at the cost of a moderate increase in the analytical and computational complexity with respect to the planar scannings, it allows the reconstruction of the antenna's complete radiation pattern, with the exception of the zones surrounding the spherical polar angles.

Two efficient probe compensated NF–FF transformation techniques with cylindrical scanning have been recently developed [1] by considering the antenna under test (AUT) as enclosed in a prolate spheroid, a shape particularly suitable to deal with elongated antennas, but which remains quite general because it contains spherical modelling as a particular case. These techniques are based on theoretical results concerning the nonredundant sampling representations of the radiated electromagnetic (EM) fields [2] and allow us to lower the number of needed NF data in a significant way, without losing the efficiency of previous approaches. As a consequence, the measurement time is considerably reduced. In the former technique (nonredundant NF interpolation plus classical NF–FF transformation), the NF data required by the standard probe-compensated NF–FF transformation with cylindrical scanning [3] are efficiently recovered via an optimal sampling interpolation (OSI) algorithm from the knowledge of a nonredundant number of samples. In the latter (direct nonredundant NF–FF transformation), the antenna far-field is directly evaluated from the nonredundant NF data without interpolating them.

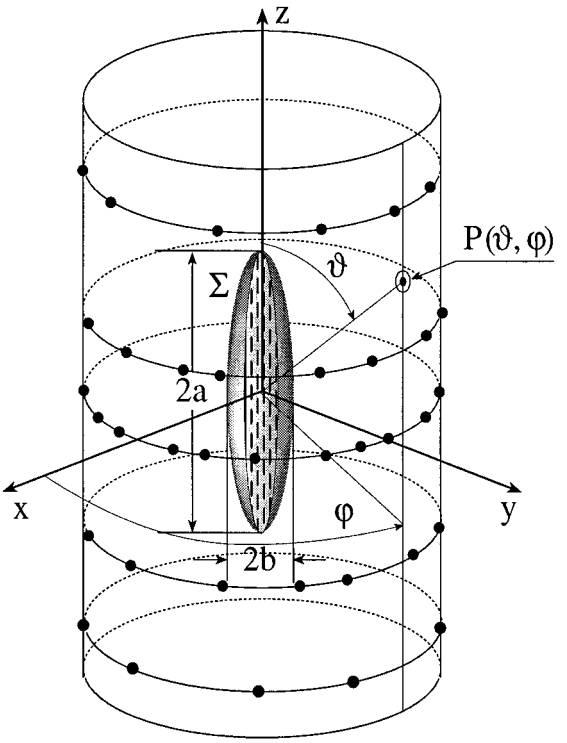

Figure 1 Geometry of the problem

It is useful to note that, due to an inaccurate control of the positioners, it may be practically impossible to obtain uniformly spaced NF measurements. On the other hand, their position can be accurately read by optical devices. Moreover, the finite resolution of the positioning devices prevents the possibility of exactly locating the probe at the points fixed by the sampling representation. As a consequence, it becomes very important to develop an efficient algorithm for an accurate and stable reconstruction of the AUT far-field from irregularly spaced NF data (see Fig. 1).

Some formulas for the direct reconstruction from nonuniform samples are available in the literature, however, they are valid only for particular sampling points arrangements, cumbersome, not user friendly, and unstable. Therefore, it is more advisable to recover the uniform samples from the irregularly spaced ones than to resort to a direct interpolation formula. In fact, once the uniform samples have been determined, the value at any point can be recovered by a proper sampling interpolation. Such an approach has been proposed to recover the uniformly distributed samples from those irregularly spaced on planar [4], cylindrical [5], or FF spherical [5] surfaces. These algorithms employ an iterative technique which converges only if there is a bi-unique correspondence between the nonuniform samples and a lattice of regularly spaced ones, which associates the nearest nonuniform one at each uniform sampling point.

Regarding the case of field reconstruction on a plane from the knowledge of the nonuniformly spaced plane-polar samples, this limitation has been overcome in [6] by developing an approach based on the use of the singular value decomposition (SVD)